

FIGURE S1

CTRL hearts

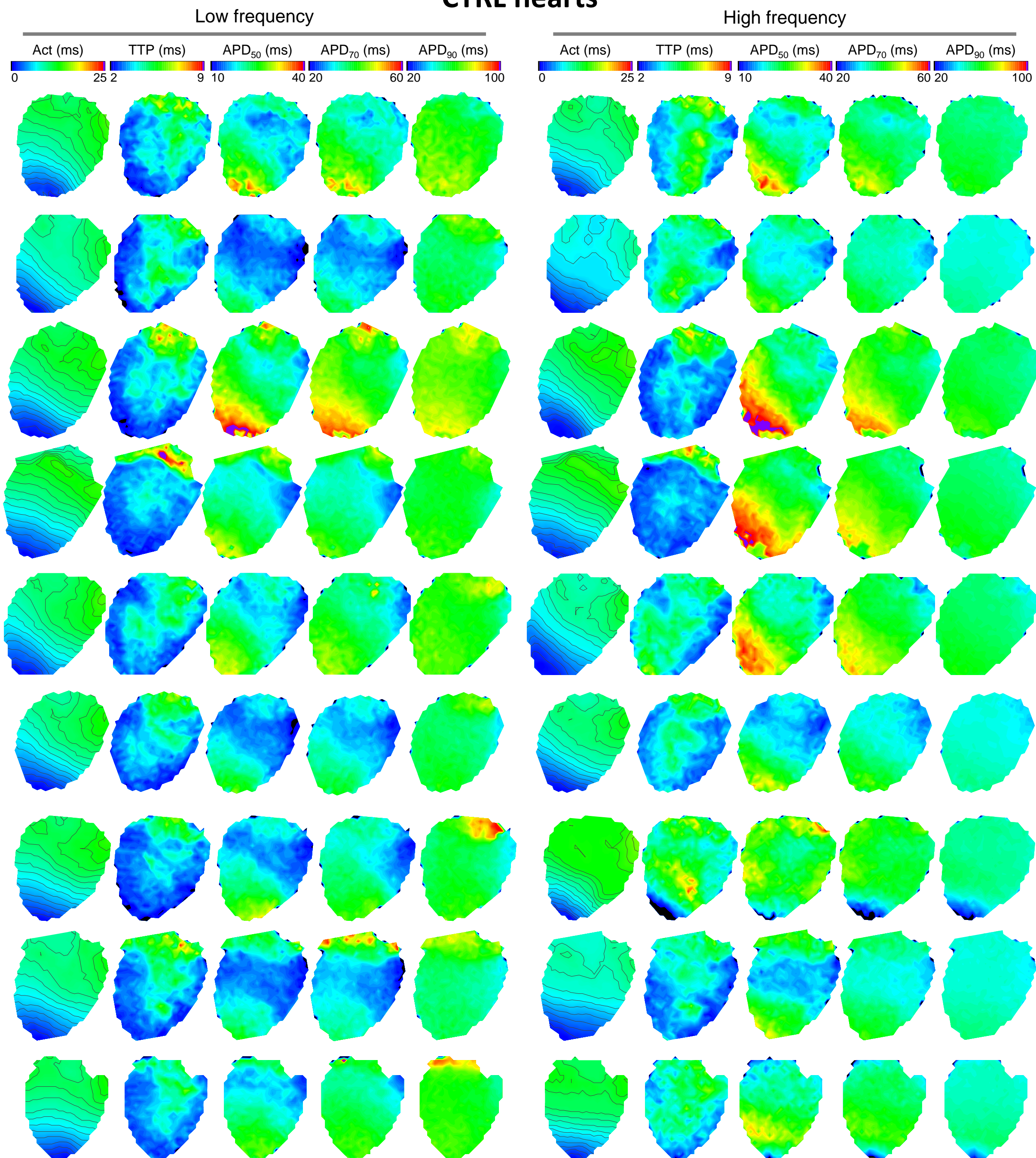


Figure S1: Left-ventricular maps of all included control (CTRL) hearts. Hearts were paced at LF (5 Hz; left panel) and HF (≥ 10 Hz; right panel). Activation time (Act) is color-coded, with isochrones of 1 ms. Time-to-peak (TTP), AP duration at 50%, 70%, and 90% of repolarization (APD₅₀, APD₇₀, APD₉₀, respectively) are color-coded with the scale indicated above. Average data obtained from these maps are included in Figure 1.

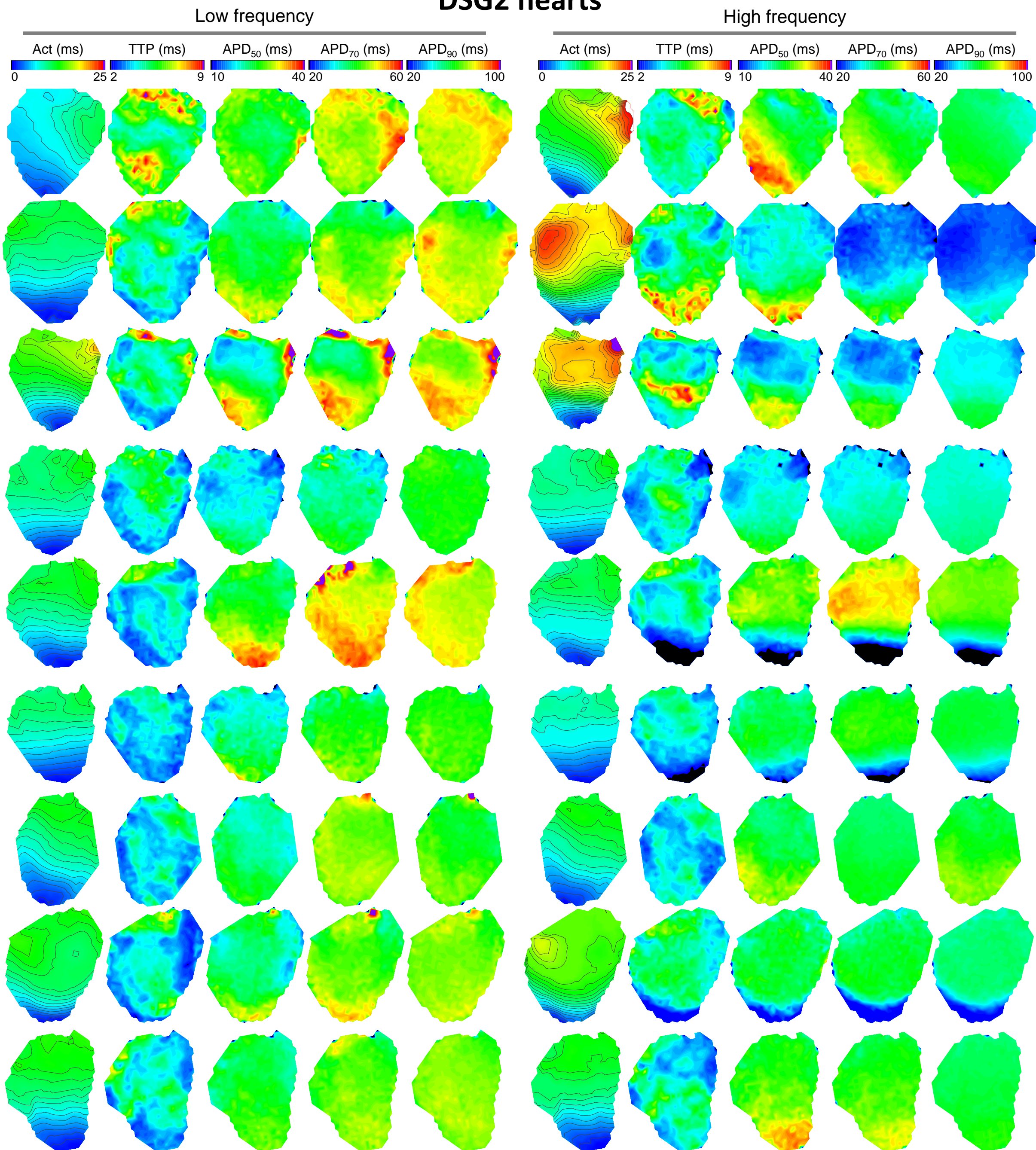
FIGURE S2**DSG2 hearts**

Figure S2: Left-ventricular maps of all included DSG2 hearts. Hearts were paced at LF (5 Hz; left panel) and HF (≥ 10 Hz; right panel). Activation time (Act) is color-coded, with isochrones of 1 ms. Time-to-peak (TTP), AP duration at 50%, 70%, and 90% of repolarization (APD₅₀, APD₇₀, APD₉₀, respectively) are color-coded with the scale indicated above. Average data obtained from these maps are included in Figure 1.

FIGURE S3

CTRL



Sarcomere lengths:

1: 2.266 μm

2: 2.238 μm

3: 2.236 μm

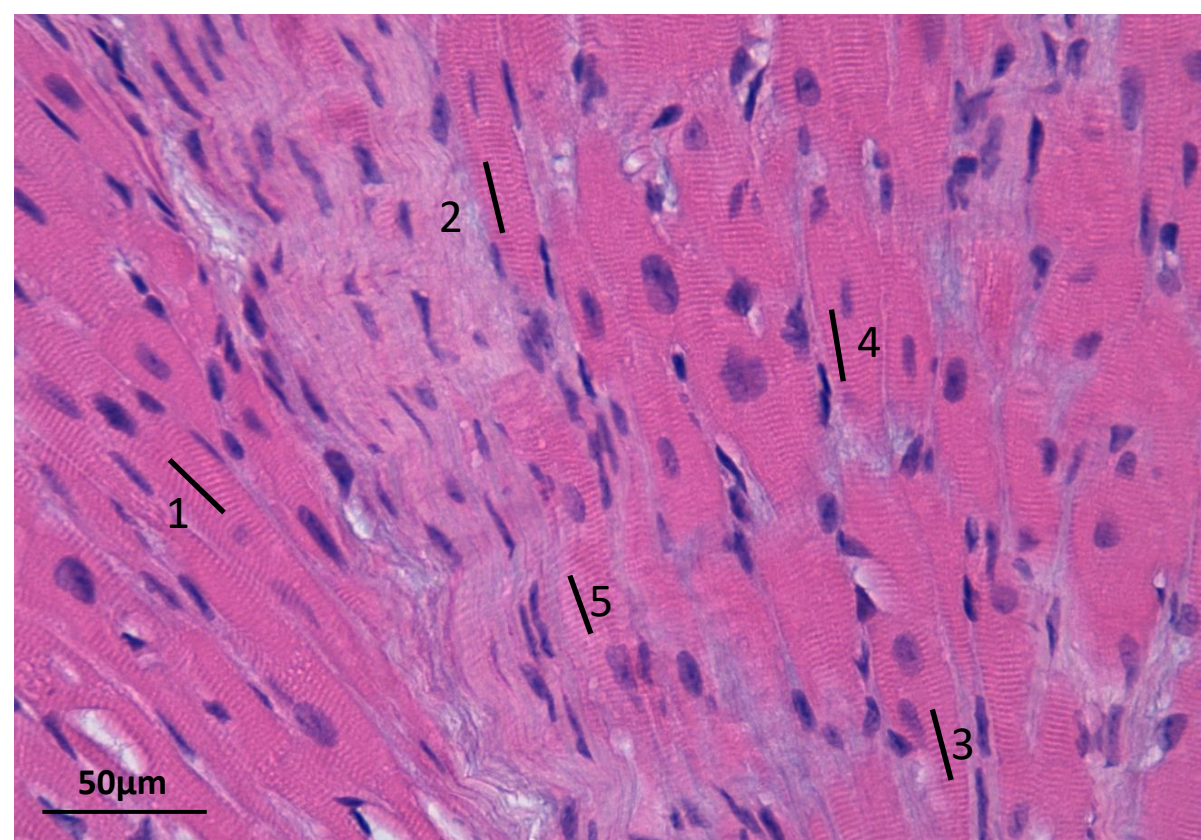
4: 2.230 μm

5: 2.248 μm

Average: 2.24 μm

Std.dev: 0.01 μm

DSG2



Sarcomere lengths:

1: 2.334 μm

2: 2.098 μm

3: 2.194 μm

4: 2.159 μm

5: 2.008 μm

Average: 2.16 μm

Std.dev: 0.11 μm

Figure S3: Tissue preservation of clearing by SHIELD protocol. Results of the histological inspection of post-clearing murine myocardium tissue from a control and a DSG2 heart, performed using haematoxylin-eosin staining. Average sarcomere length (black lines, ten consecutive sarcomere z-lines) was measured by selecting cells with their major axis as parallel as possible to the image plane, in order to minimize estimation errors of sarcomere length (SL) caused by cell tilt in 3D space (cosine-error).

FIGURE S4

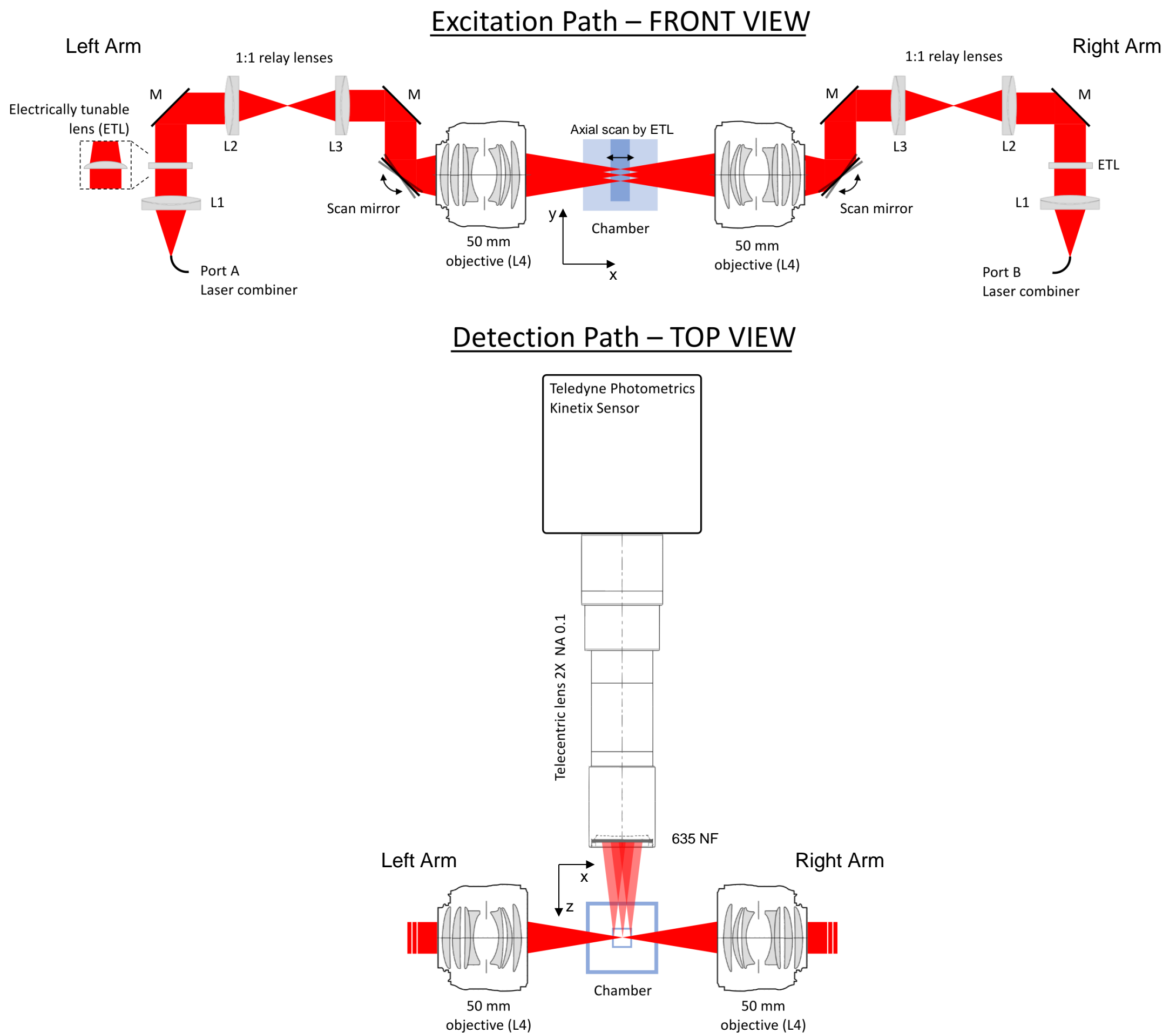


Figure S4: MesoSPIM optical scheme. L1: Achromatic doublets (AC254-050-A-ML, Thorlabs), ETL: Electrically Tuneable Lens (EL-16-40-TC-VIS-5D-1-C, Optotune), M: Dielectric Mirror (BBE1-E02, Thorlabs), L2 and L3: Achromatic doublets (G063200000, Qioptiq), Scanning mirror (GVS211/M, Thorlabs), L5: Camera objective (Nikkor AF-S 50mm f/1.4G, Nikon), 650 NF: NF03-405/488/561/635E-25, StopLine quad-notch filter, Semrock.

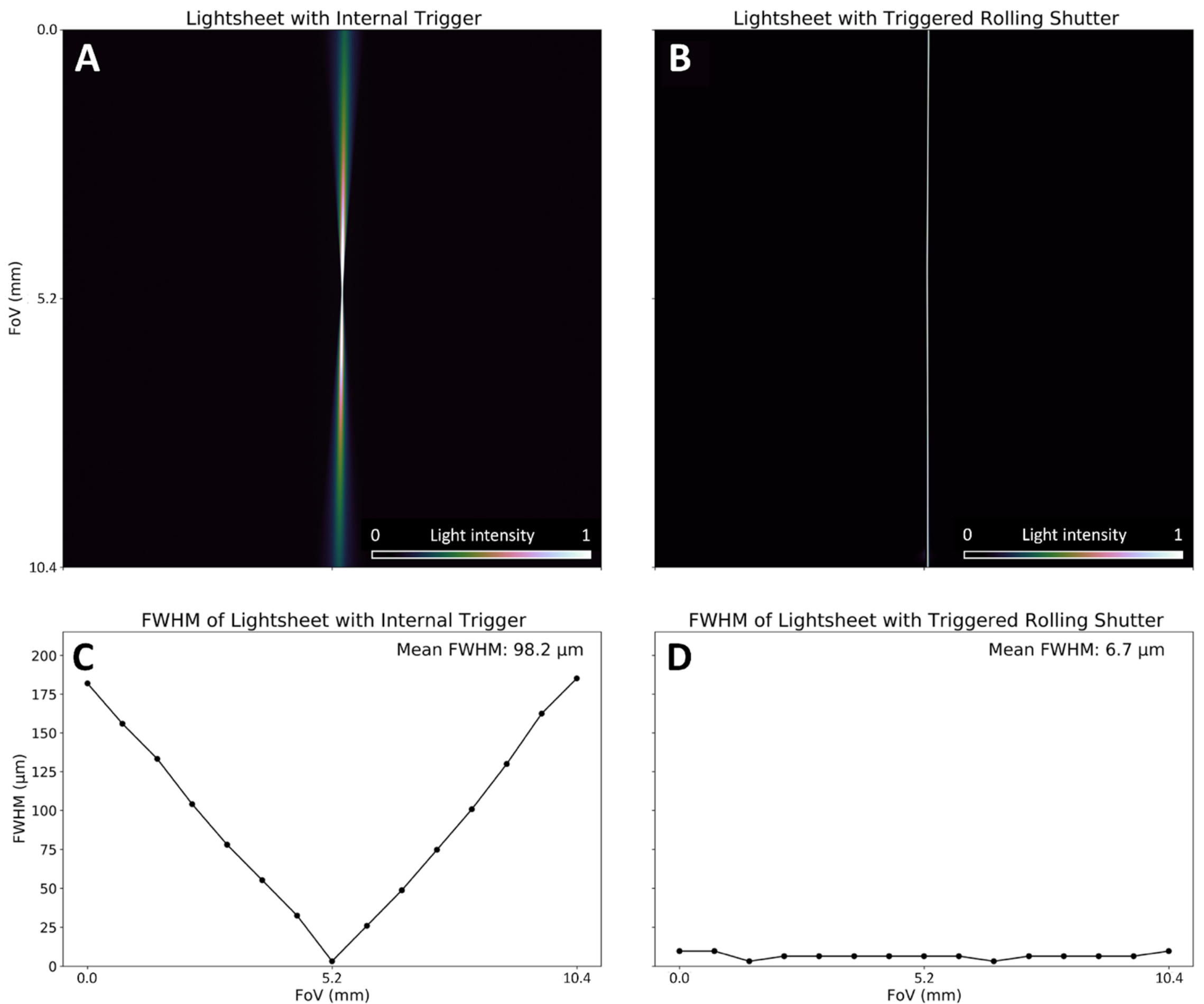
FIGURE S5

Figure S5: MesoSPIM light-sheet generation. (A, B) Excitation light-sheet statically focused into the centre of Field of View (A) and dynamically generated by the synchronization between the camera rolling shutter (operating at 1.92 Hz) and the scanning light-beam driven by the tunable lens (B). Pixel size: 3.25 μm ; exposure time: 10 ms; light source: 638 nm; light intensity is normalized and reported with a colormap. The Full Width at Half Maximum (FWHM) of the light intensity profile is evaluated in 15 different positions along the FoV of panel A and B; results and averages are shown in panel C and D, respectively.

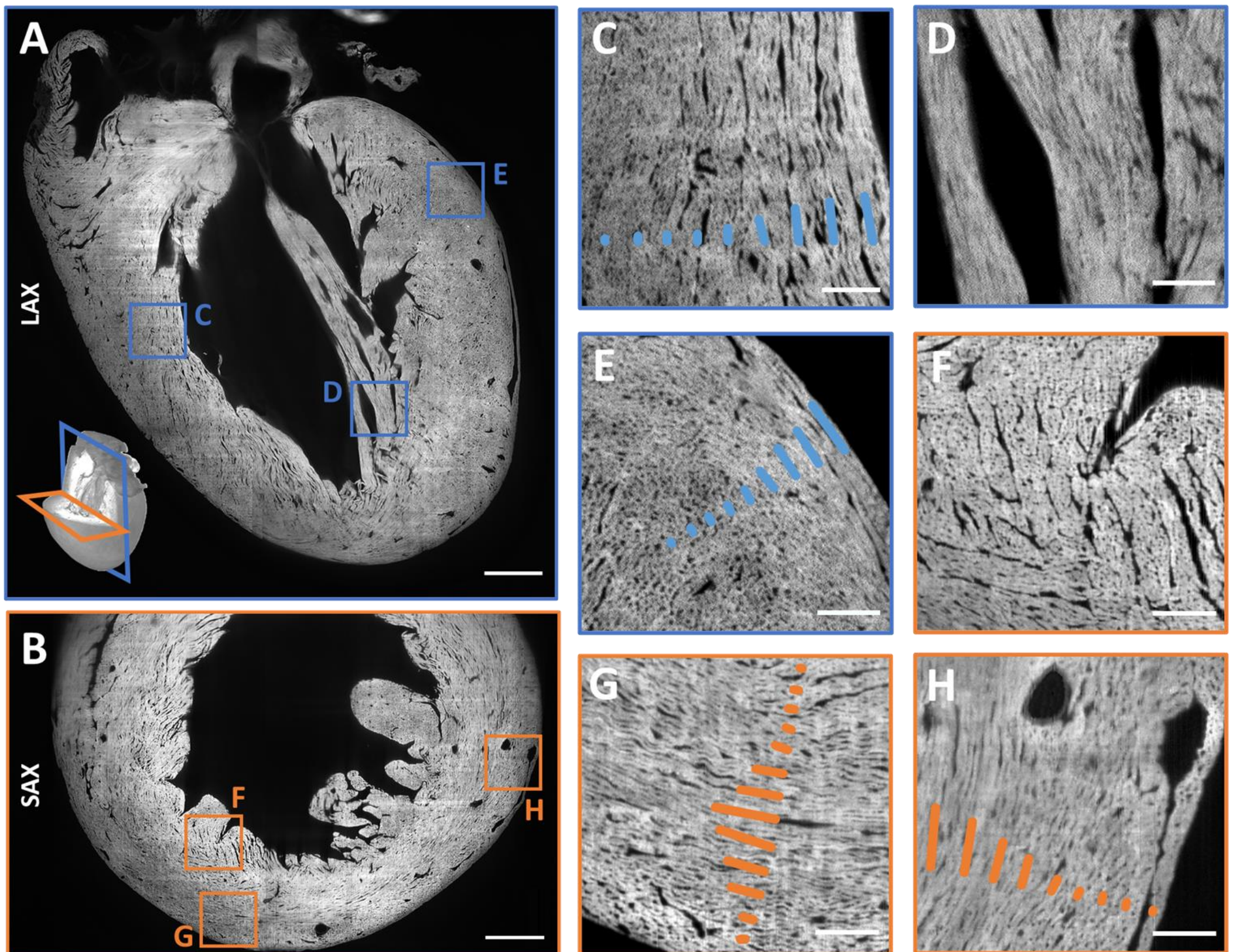
FIGURE S6

Figure S6: Resolving cellular orientation in the entire heart. High-resolution reconstructions by fluorescence signal of cardiac muscle of a cleared healthy heart, collected by mesoSPIM. (A, B) The long axis (LAX) plane and Short Axis (SAX) plane sections are shown. Main cellular orientation is well resolved in both LAX and SAX views, enabling detection of cellular alignment following the helical angle distribution in the myocardial wall (highlighted in C, E, G, and H panels). Cells can be resolved also in the trabeculae inside the cardiac chamber (panels D, F). Pixel size: $3.25\ \mu\text{m} \times 3.25\ \mu\text{m}$. Scale bar: 1 mm (left panels), $200\ \mu\text{m}$ (C-H inserts).

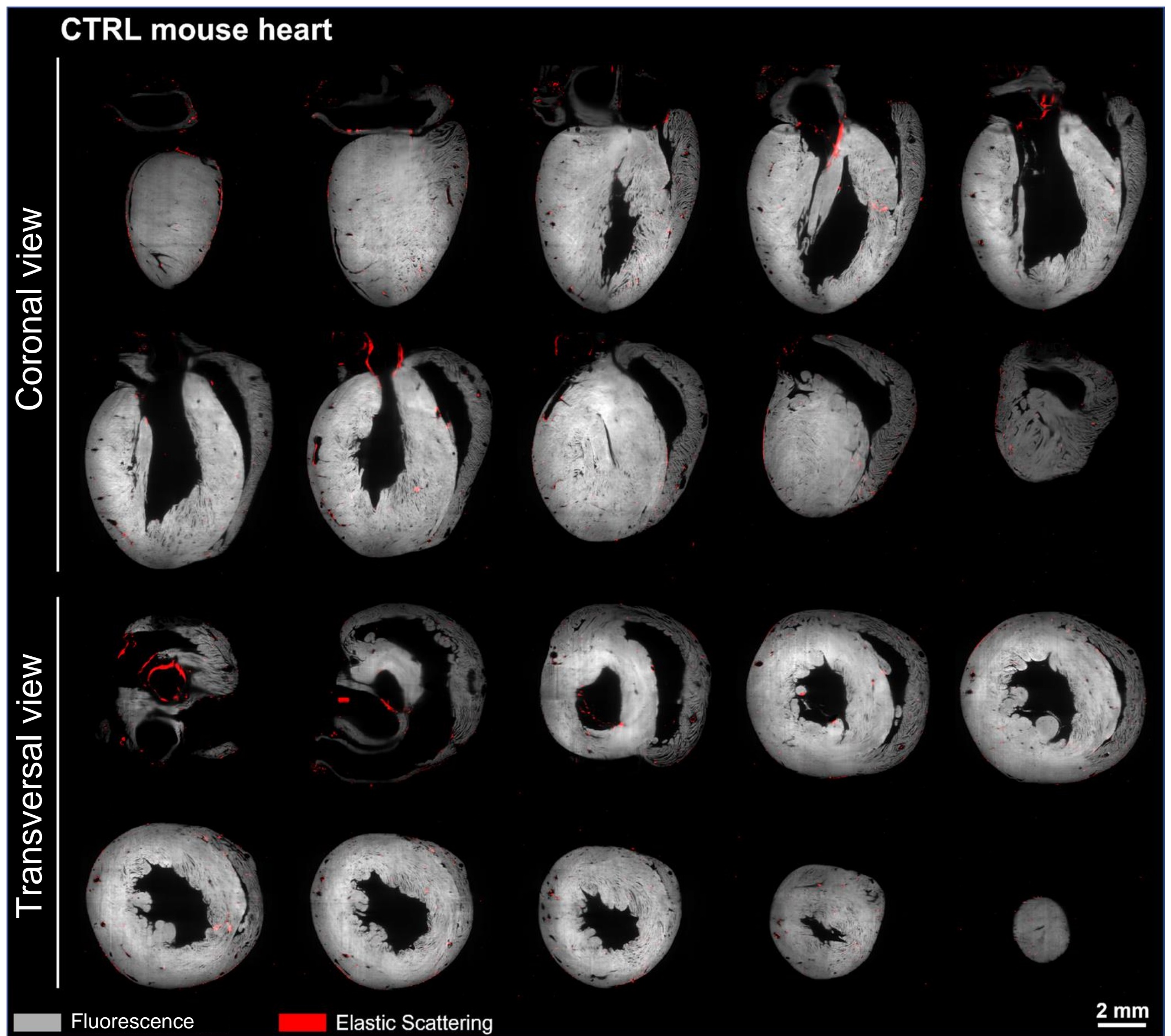
FIGURE S7

Figure S7: MesoSPIM tomography of a cleared murine heart. A representative whole-heart reconstruction of a healthy mouse heart performed following the optimized SHIELD clearing protocol and the MesoSPIM-based imaging protocol. For each heart, two identical reconstructions were acquired, both with and without the long-pass filter ($\lambda > 650$ nm) to collect tissue fluorescence (here represented with a grey signal) and elastic scattering (red signal), respectively. Original images voxel size: $3.25 \mu\text{m} \times 3.25 \mu\text{m} \times 3.1 \mu\text{m}$; two-channels whole-heart tomography voxel size: $6 \mu\text{m} \times 6 \mu\text{m} \times 6 \mu\text{m}$.

FIGURE S8

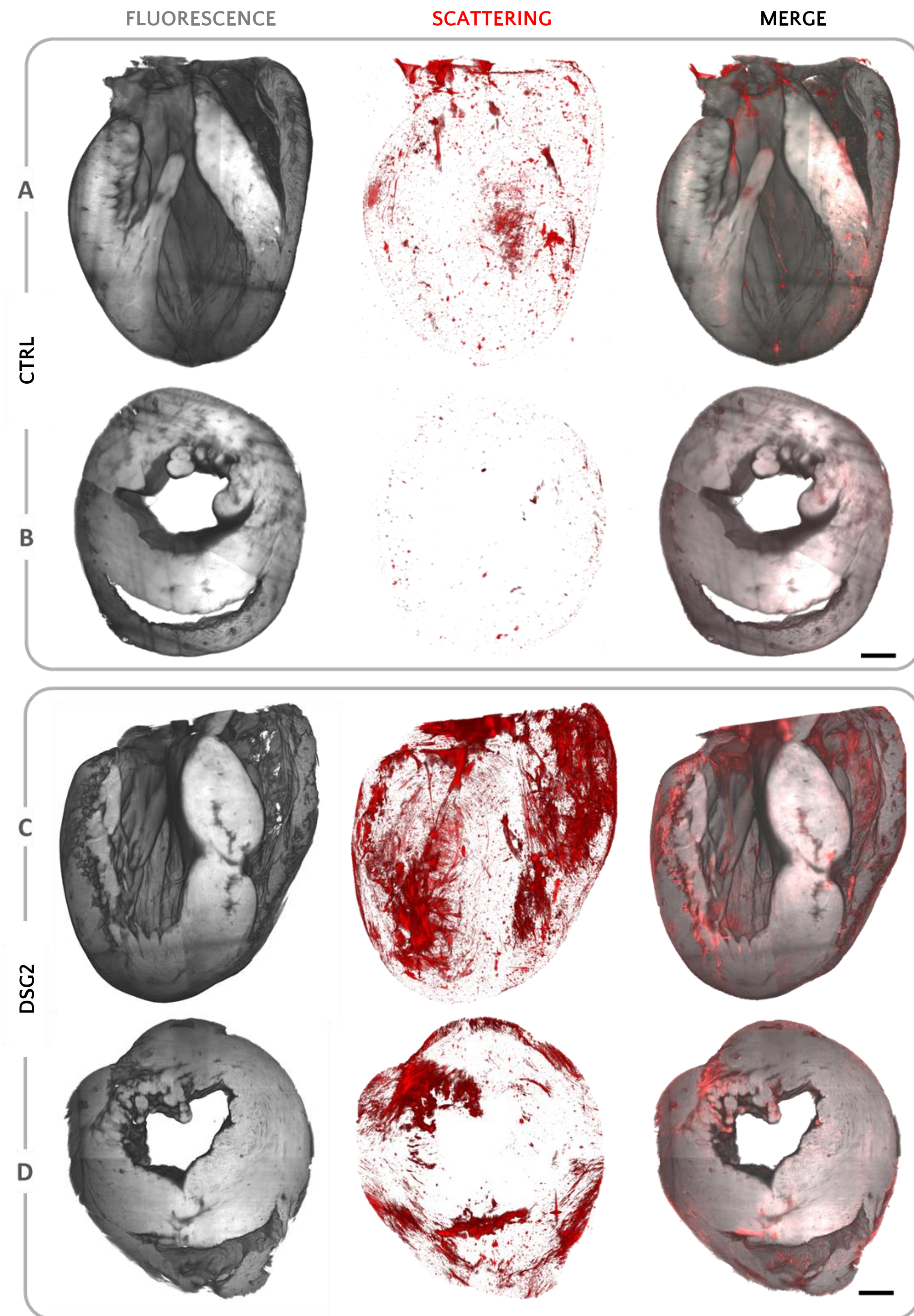
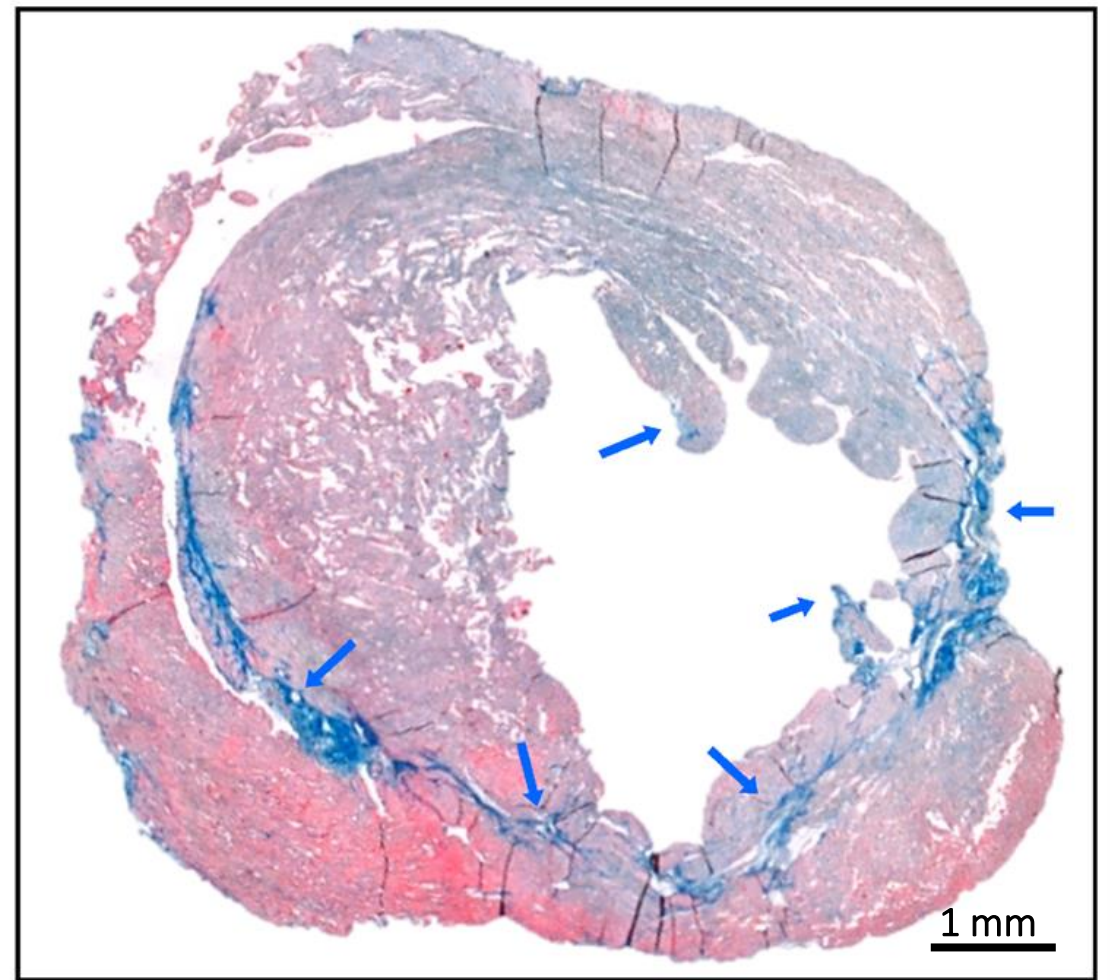
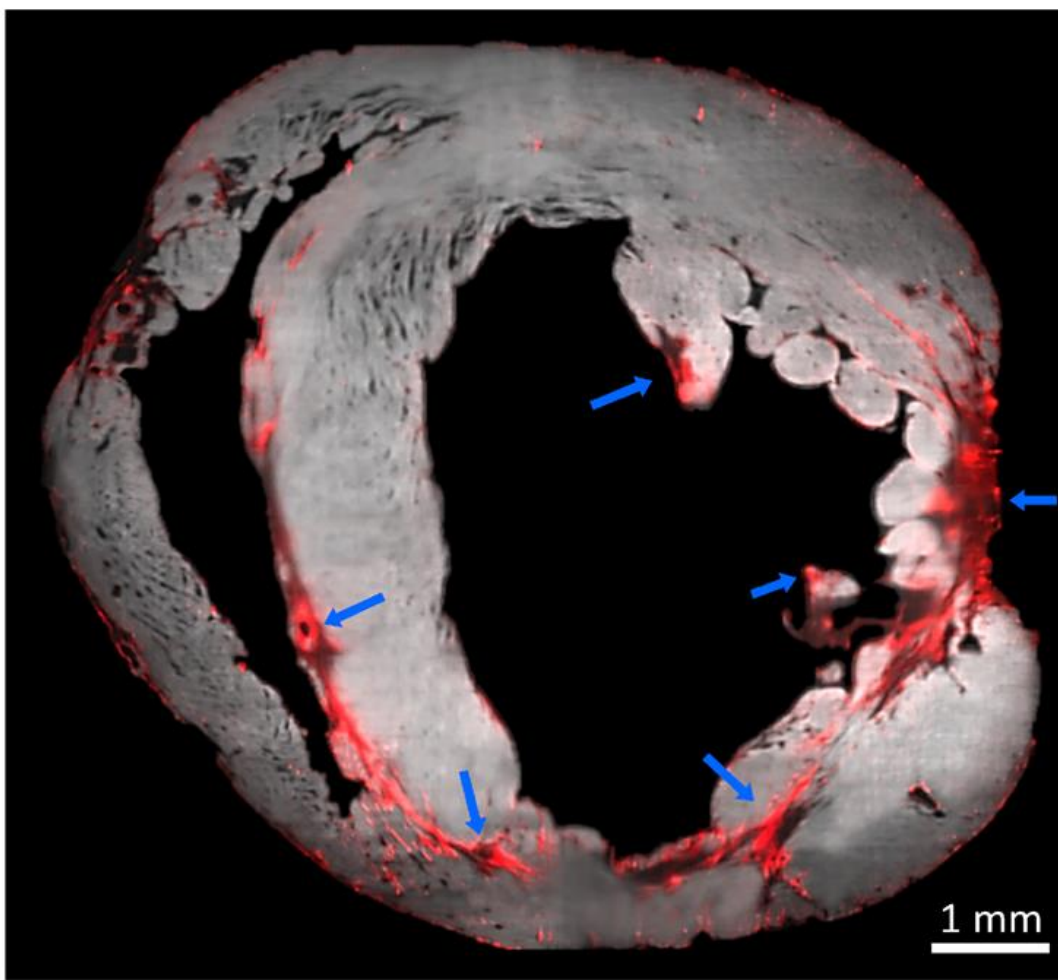


Figure S8: Mouse whole heart reconstruction. Coronal (A, C) and transversal (B, D) views of three-dimensional reconstructions of cleared CTRL and DSG2 entire hearts by mesoSPIM. Three-dimensional reconstructions are generated with an isotropic voxel size of $6\ \mu\text{m}$ from original images (pixel size of $3.25\ \mu\text{m} \times 3.25\ \mu\text{m} \times 3.1\ \mu\text{m}$ in XYZ) and rendered with ImageJ software. The final reconstructions (on the right) are generated by merging fluorescence (myocardium) and scattered light (collagen). Scale bars: 1 mm.

FIGURE S9

MESOSPIM

MASSON'S TRICHROME



ARRHYTHMOGENIC MOUSE





FLUORESCENCE  =  MYOCARDIUM
SCATTERING  =  COLLAGEN

Figure S9: Validation of scattering signal. On the left, a virtual section of a mesoSPIM-based tomography of a DSG2 mouse heart, where fluorescence signal (in grey) and scattering signal (in red) are shown. On the right, a Masson's trichrome staining of the correspondent semi-final histological section of the same heart highlights myocardial tissue (in pink) and collagen deposition (in blue). Histology confirms the accuracy of the proposed scattering-based approach to detect fibrotic areas (blue arrows).

FIGURE S10

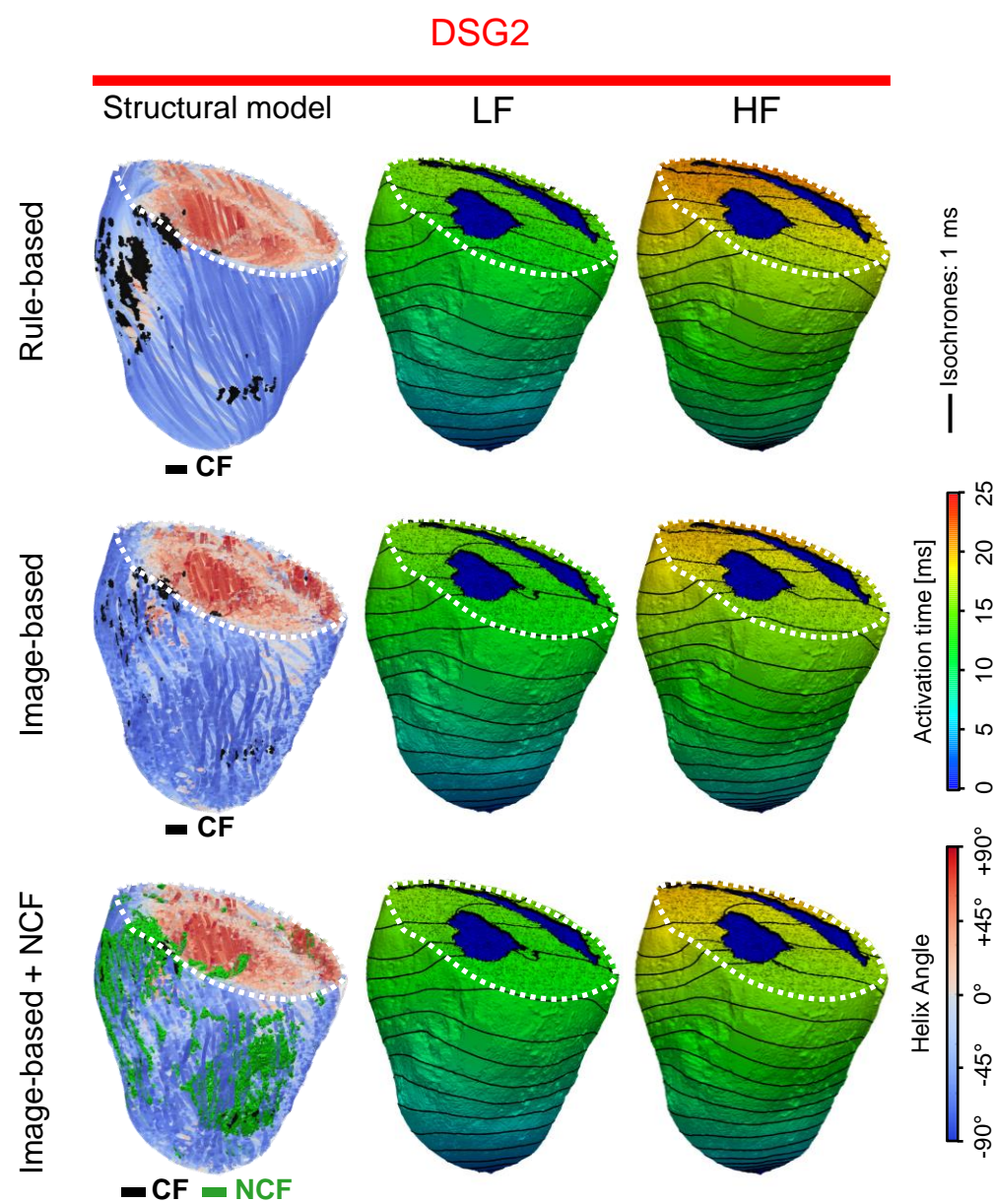


Figure S10: Integrated computational modelling of AP propagation.

Electrical propagation upon apical pacing at LF (5 Hz) or HF (15 Hz) simulated by a functional model of electrical activity in one DSG2 heart (second row in Fig S17). Structural information was integrated into a bi-ventricular geometrical model (spatial resolution: 100 μm) based on myocardium anatomy and compact fibrosis (CF) at three progressive levels: a theoretical distribution of cardiomyocytes (rule-based), real cardiomyocytes organisation (image-based), and after adding non-compact fibrosis (NCF) distribution. The figure show the 3D activation maps of the last beat (after 10 pulses at LF and HF) are aligned to experimental data presented in Fig. S17. Ventricular cavity orifice was shown in blue for better visualization.

FIGURE S11

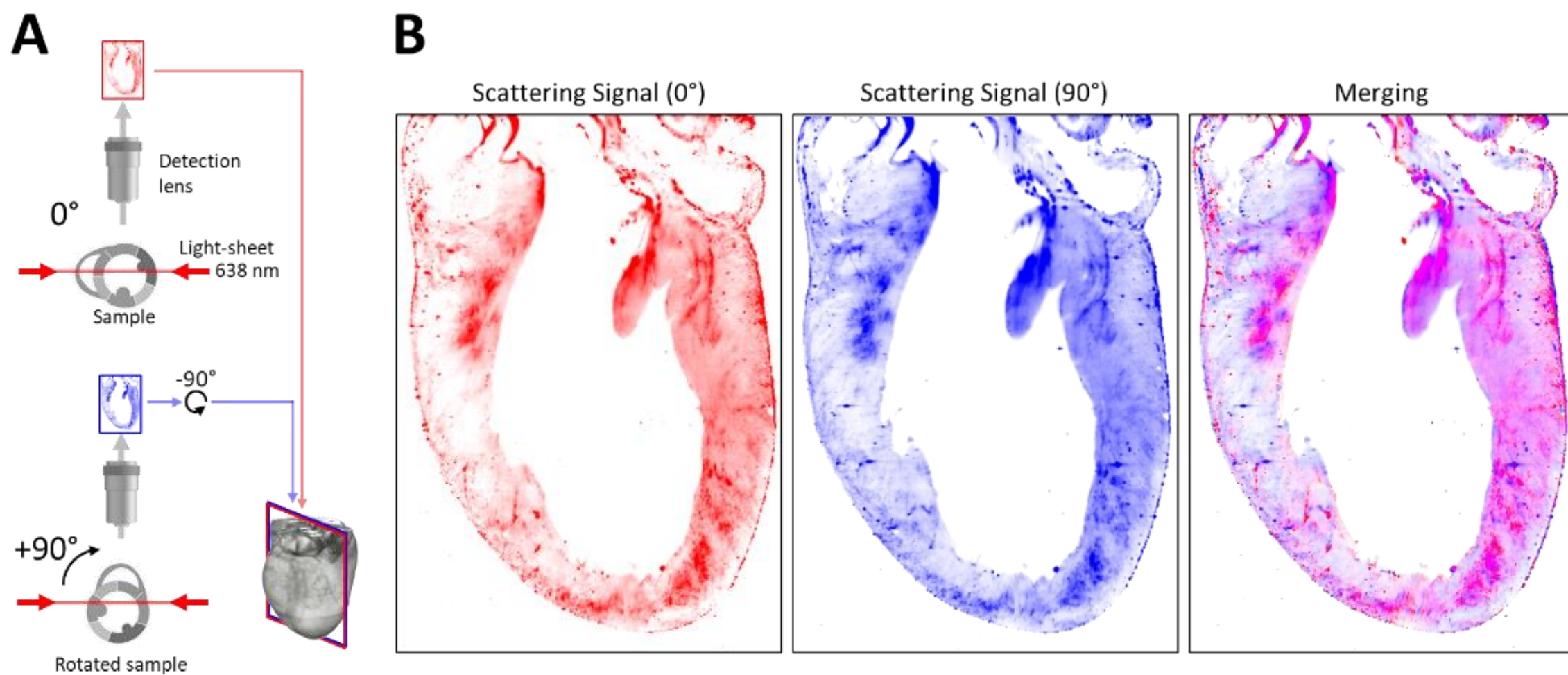


Figure S11: Scattering signal independency from excitation direction. (A) Schematic diagram of the excitation and detection paths in two perpendicular configurations. (B) Representative tomographic internal sections of the scattering signal of the same heart, collected at 0° and 90° and subsequently realigned, both separated and merged.

FIGURE S12

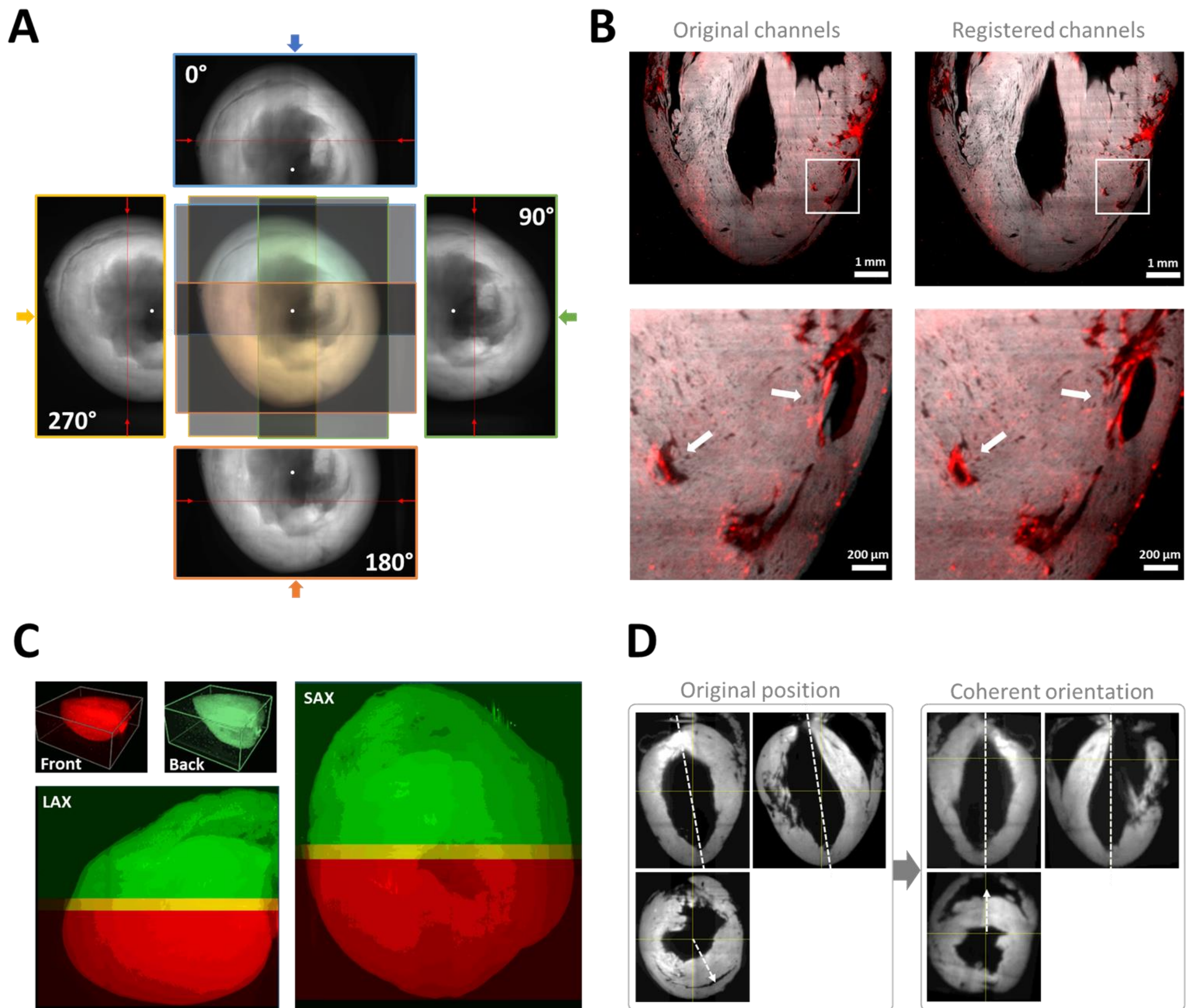


Figure S12: Sample imaging and image preprocessing. (A) Schematic of multiple acquisitions performed to reconstruct an entire cleared mouse heart with the mesoSPIM setup. Partial tomographies were performed for each rotation of the organ around its long axis (white spots superimposed on Short-Axis Average-Intensity-Projections) at 0°, 90°, 180°, and 270° degree (blue, green, orange and yellow arrows indicate the optical axis). Red lines represent the optical sectioning plane of the light-sheet generated by a light source set at 638 nm from two parallel excitation arms (red arrows). In the center, the sample shape is reassembled by merging the four views as an example. (B) Result of the 3D channel registration process performed on a representative mouse heart reconstruction (muscle fluorescence in grey, scattering light in red) with the FijiYama plugin (ImageJ) to correct the spatial shift (white arrows) between channels. (C) Registration of two opposite partial tomographies (front and back) of a reconstruction using Huygens Professional (SVI). After the initial manual registration, the software optimizes the alignment and fuse the 3D images. (D) Representative example of manual three-dimensional realignment performed on all reconstructions. The sample is rotated iteratively on each view of the 3d tomography to re-align the long axis of the organ and place the right ventricle on top of the SAX view.

FIGURE S13

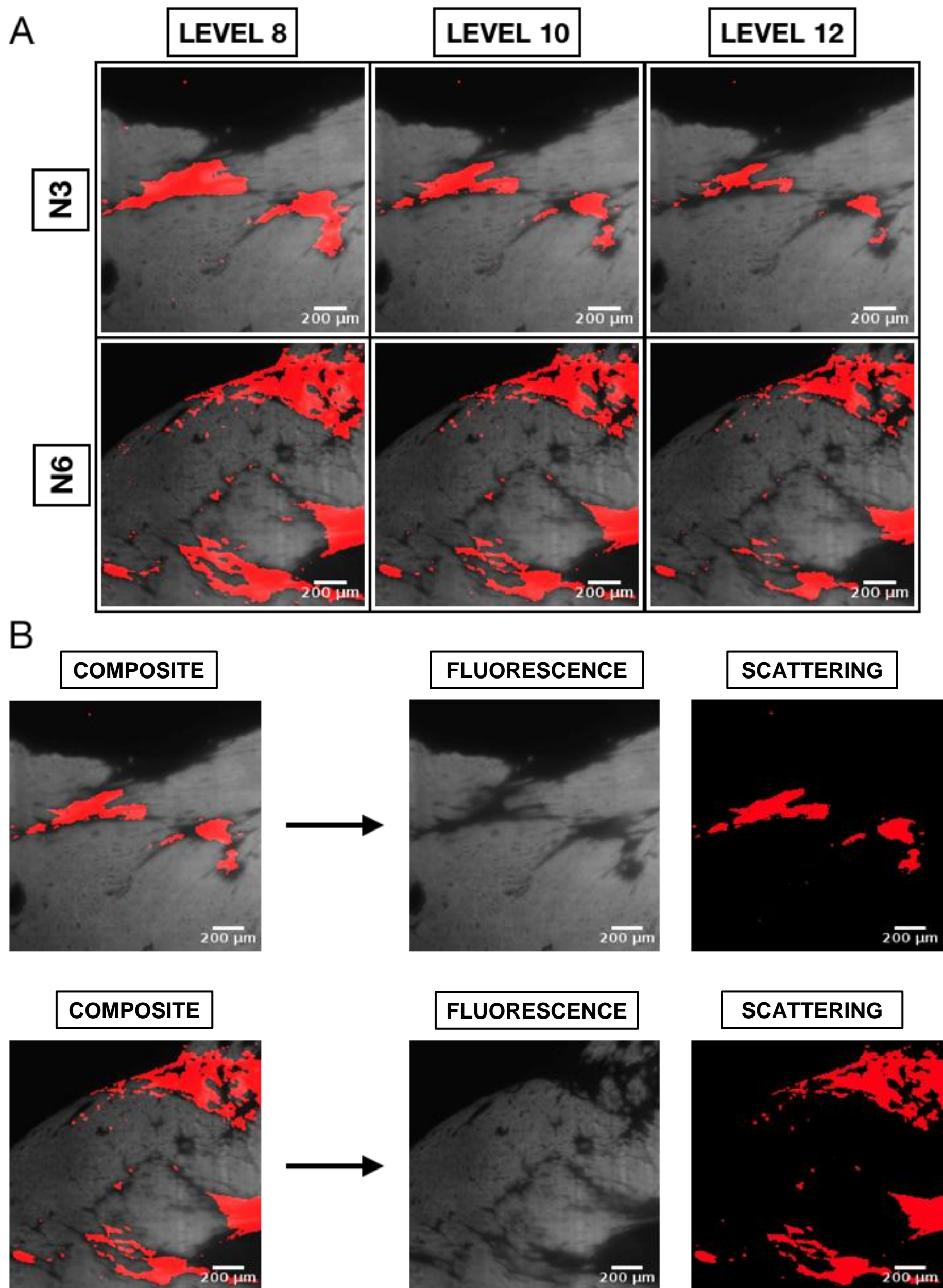


Figure S13: Optimization of threshold-based segmentation of compact fibrosis from scattering signal. (A) Segmentation of compact fibrosis (CF) from scattering signal in regions of interests (ROIs) of two different DSG2 hearts (N3 and N6), varying the threshold of pixel intensity (level of gray, LEVEL). (B) Same ROIs shown in panel A, for intensity level = 10, showing the fluorescence and the scattering channels separately.

TABLE S1

| HEART | TH | MYOCARDIUM VOL. | COLLAGEN VOL. | PERCENTAGE |
|--------------|-----------|------------------------|----------------------|-------------------|
| CH1 | 6 | 208.13 mm ³ | 5.07 mm ³ | 2.43 % |
| CH2 | 5 | 237.74 mm ³ | 6.11 mm ³ | 2.57 % |
| CH3 | 7 | 266.65 mm ³ | 6.90 mm ³ | 2.59 % |
| CH4 | 8 | 212.28 mm ³ | 5.34 mm ³ | 2.52 % |
| CH5 | 6 | 269.51 mm ³ | 4.71 mm ³ | 1.75 % |
| CH6 | 7 | 232.08 mm ³ | 4.82 mm ³ | 2.08 % |
| CH7 | 8 | 215.20 mm ³ | 4.03 mm ³ | 1.87 % |
| CH8 | 5 | 230.16 mm ³ | 5.14 mm ³ | 2.23 % |
| CH9 | 6 | 243.37 mm ³ | 5.04 mm ³ | 2.07 % |

Table S1: Optimization of thresholding levels for collagen segmentation in CTRL hearts. For each control heart (CH), the threshold value (TH) used to segment collagen from scattering signal is reported, with the myocardium and the resulting collagen volumes. Threshold values were selected to fit an average percentage of segmented collagen in the organ of about 2 - 2.5%, as reported in literature (PMID: 33963238; PMID: 19762097).

FIGURE S14

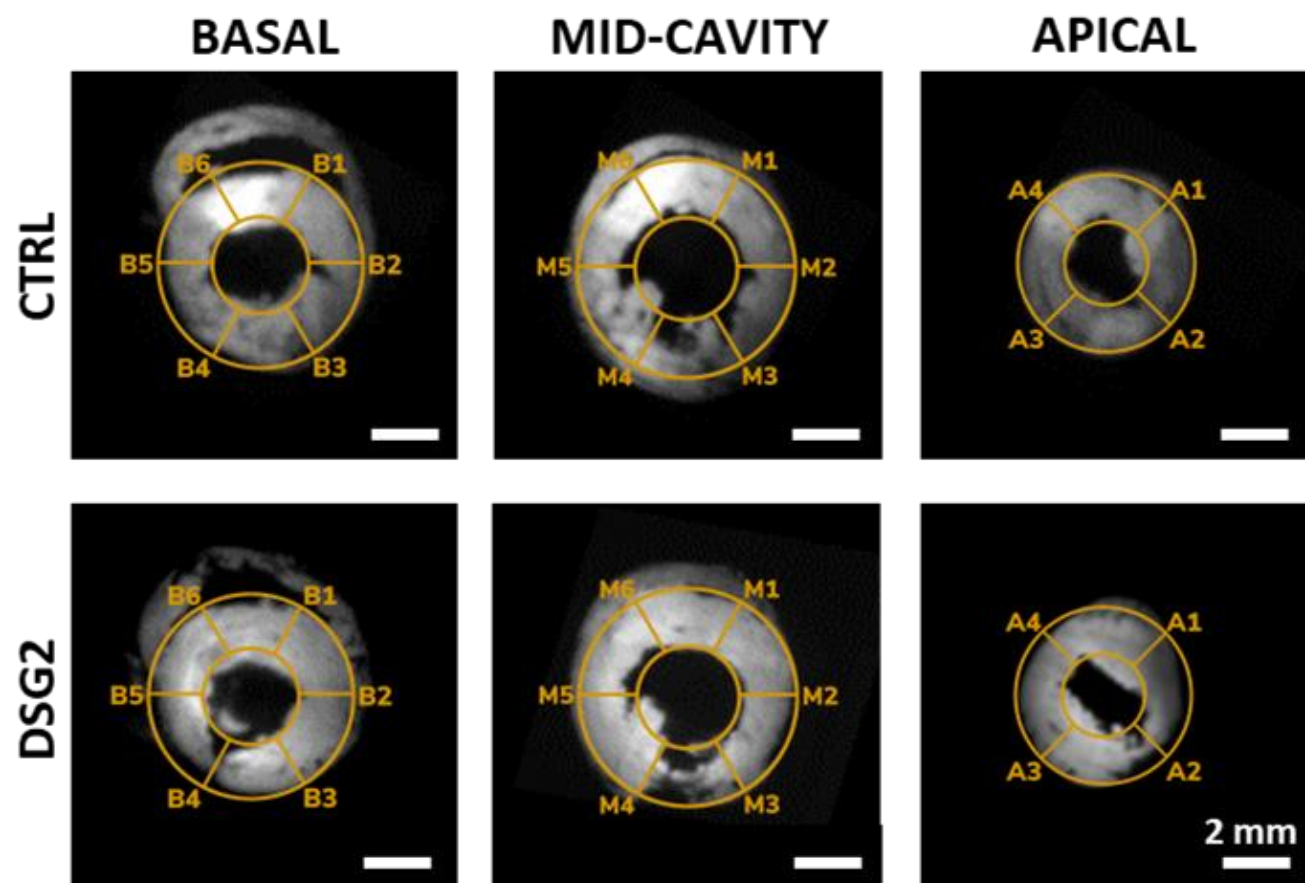


Figure S14: Reference system for anatomical measurements of the Left Ventricle wall thickness. Representative Short-Axis views of fluorescence signal (in grey) of CTRL and DSG2 heart reconstructions used to measure LV wall thickness following the AHA seventeen-segments standard protocol (superimposed in yellow).

FIGURE S15

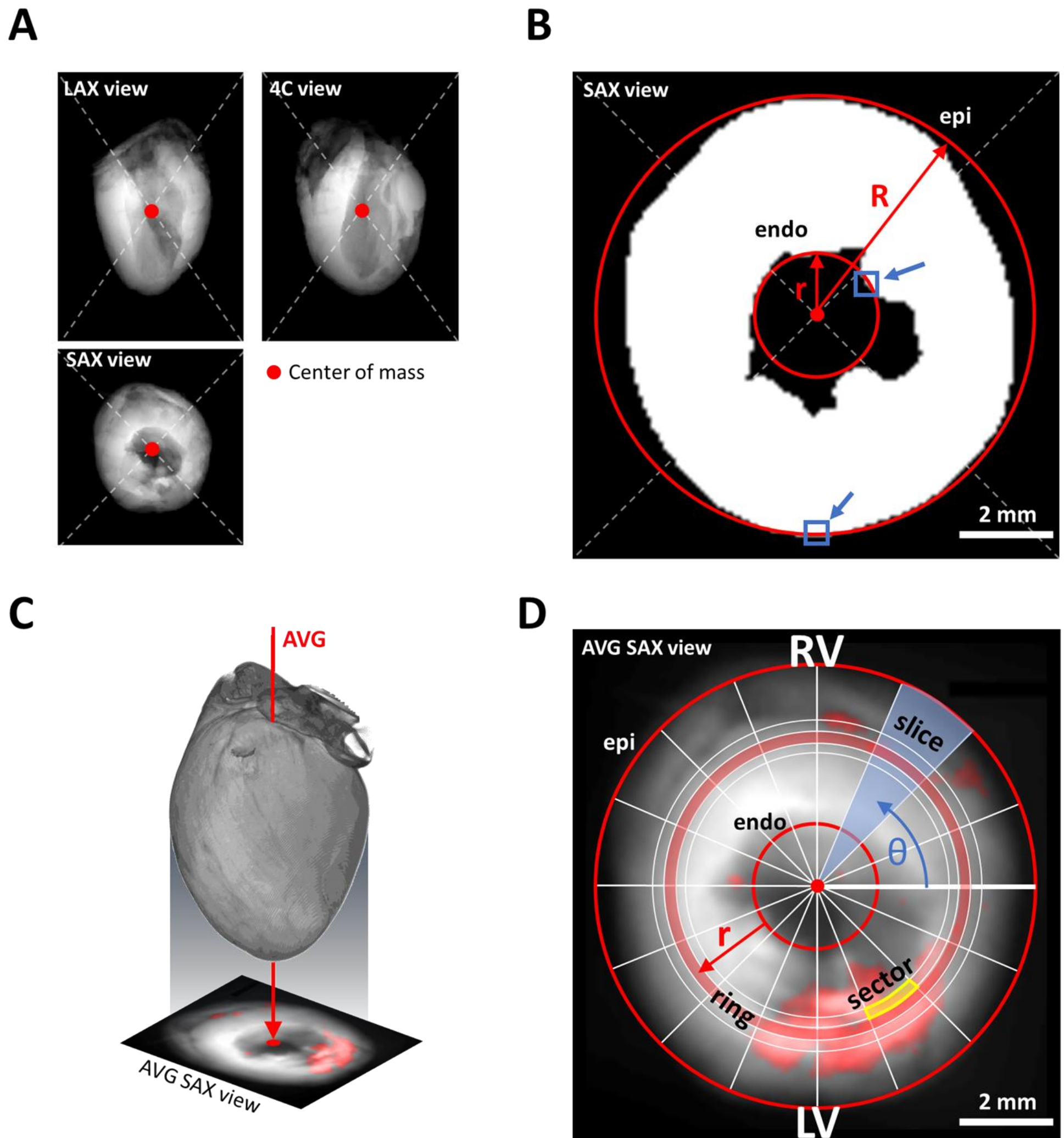


Figure S15: Automatic spatial quantization of 3d data around LV wall. Representative schematics of the main steps of automatic quantization software developed to analyze the spatial distribution of fibrosis around LV wall in 3D segmentations. (A) The myocardium is centered in the 3d volume by evaluating the barycenter of the fluorescence signal. (B) The radii of circles that fit endocardium (r) and epicardium (R) surfaces are estimated matching smaller and bigger circumferences touching a pixel (blue arrows) of the myocardium segmentation in the central SAX view. (C) Segmentations were averaged along the main axis of the hearts, generating an average SAX (AVG SAX) view. (D) Angular and radial quantizations of the AVG SAX view are performed with sixteen incremental angles and sixteen incremental radii, respectively. The sum of the signal inside each sector is stored in a normalized LV map. Abbreviations: LAX: long-axis view, SAX: short-axis view, 4C: four-chamber, epi: epicardium, endo: endocardium, LV: left ventricle, RV: right ventricle, AVG: average.

FIGURE S16

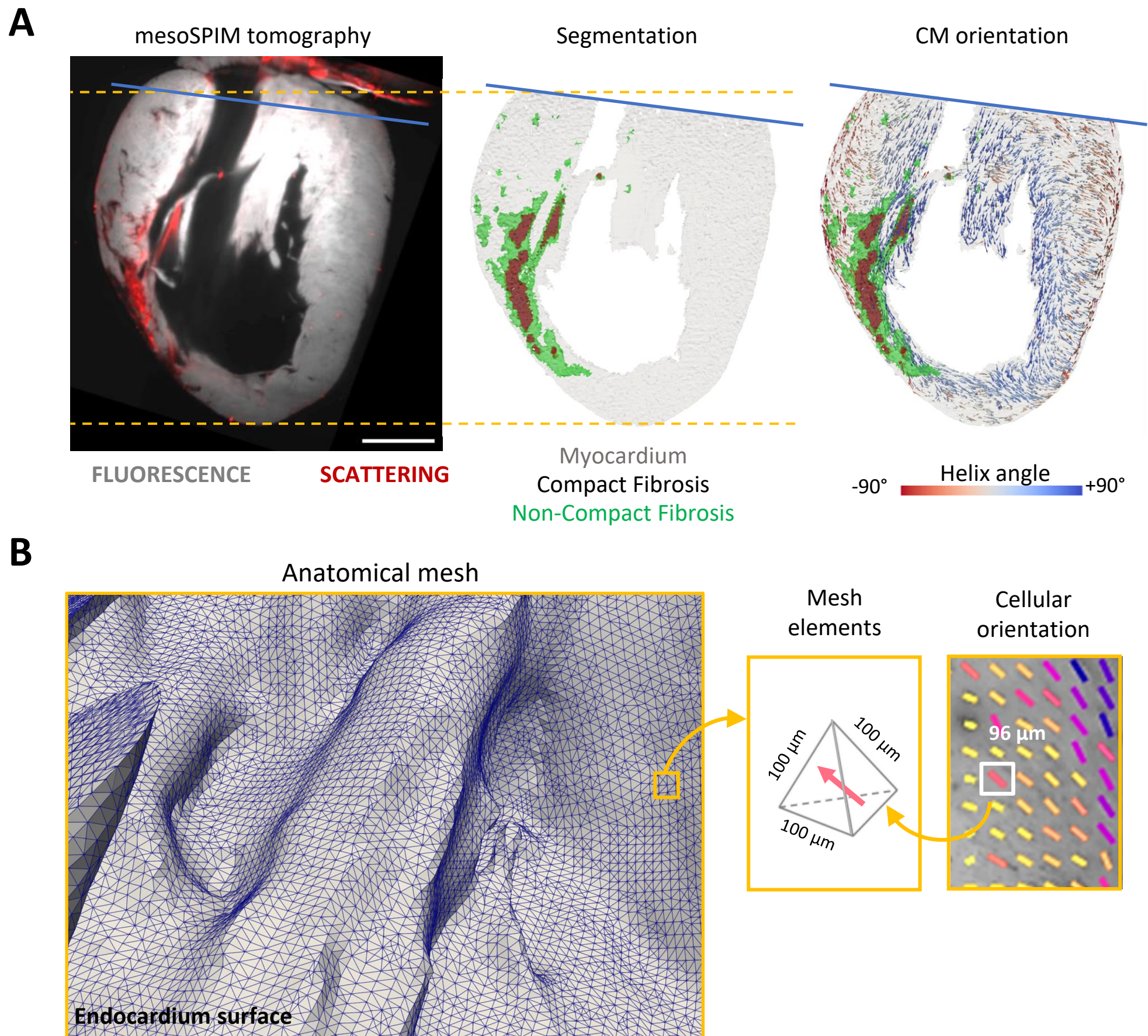


Figure S16: Integrated anatomical model. (A) Workflow of integrated anatomical model generation. (B) Zoom of the endocardial surface of an anatomical model of a mouse heart, generated by the segmentation of mesoSPIM images. A single mesh element is represented by a tetrahedron, within which the local orientation of cardiomyocytes, extracted from the analysis of the myocardial fluorescence signal, is integrated.

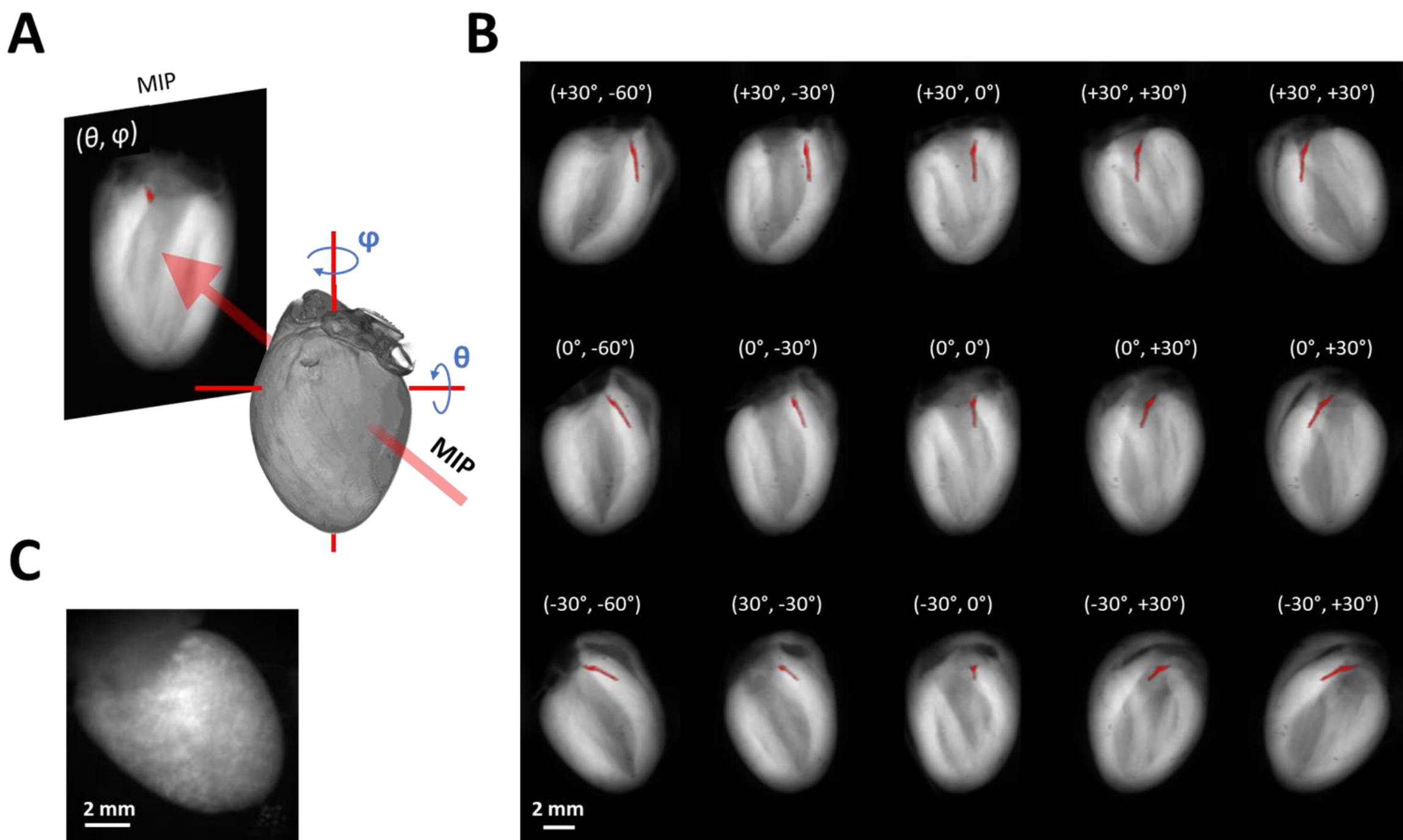
FIGURE S17

Figure S17: Automatic rotation of mouse heart tomographies for morpho-functional maps correlation. (A) Schematic of the automatic software tool used to create Maximum Intensity Projections (MIP) of whole mouse heart tomographies, previously finely rotated around the long axis (with θ) and transversal axis (with ϕ). (B) Representative example of MIPs of a mouse heart tomography containing fluorescence (grey) and scattering signal (red) for each couple of rotations (θ , ϕ) at -60° , -30° , 0° , 30° , and 60° . In the figure, the scattering signal related to the big vessel is used as a reference. (C) Representative example of a fluorescent signal image of a Langendoff-perfused mouse heart during the optical mapping protocol.